5 Charge Formation and Delocalization

Table of Contents

5.1 Solitons

- Peierls' theory: one dimensional equally spaced lattice with one electron per ion is unstable

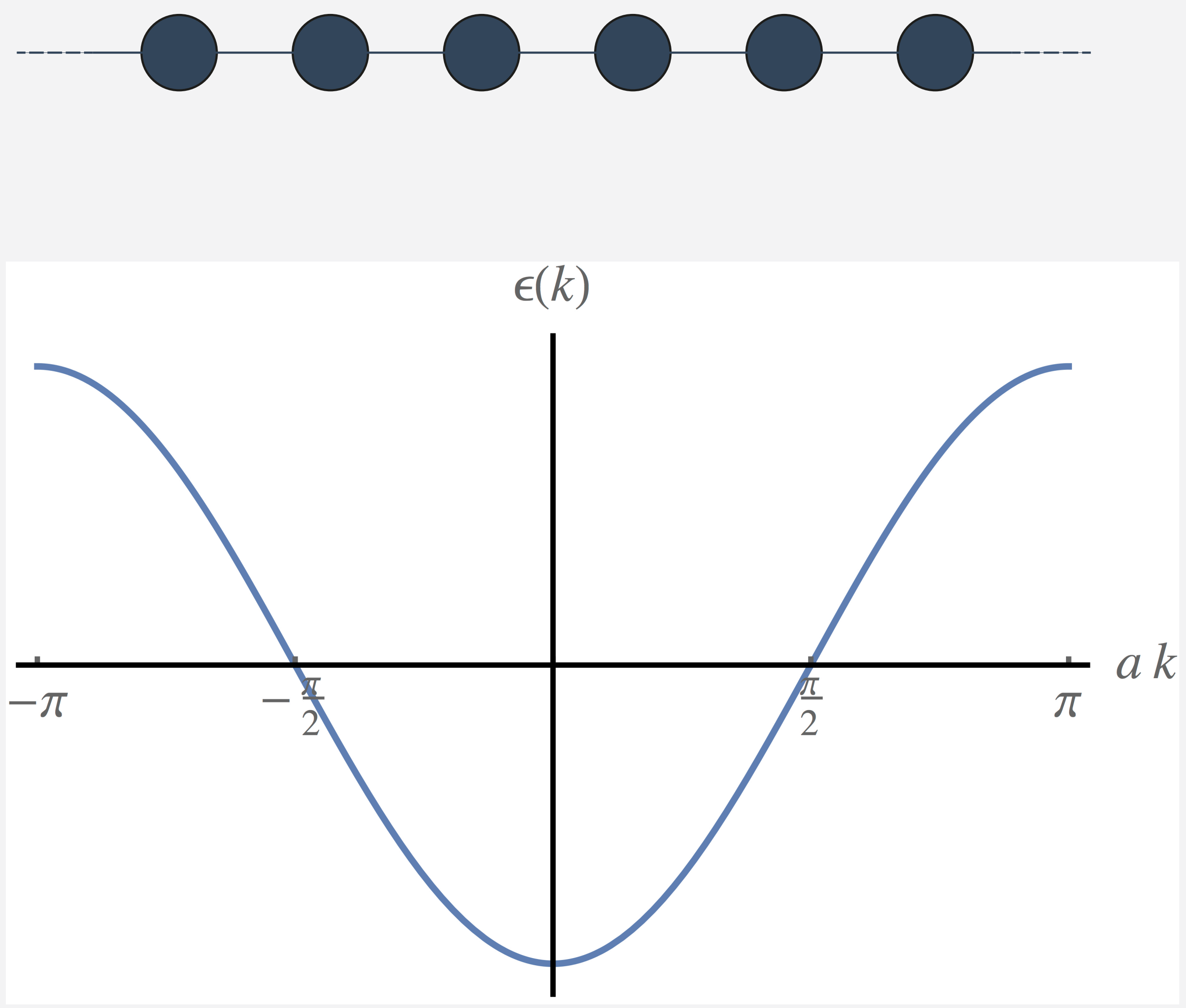

undistorted 1D lattice

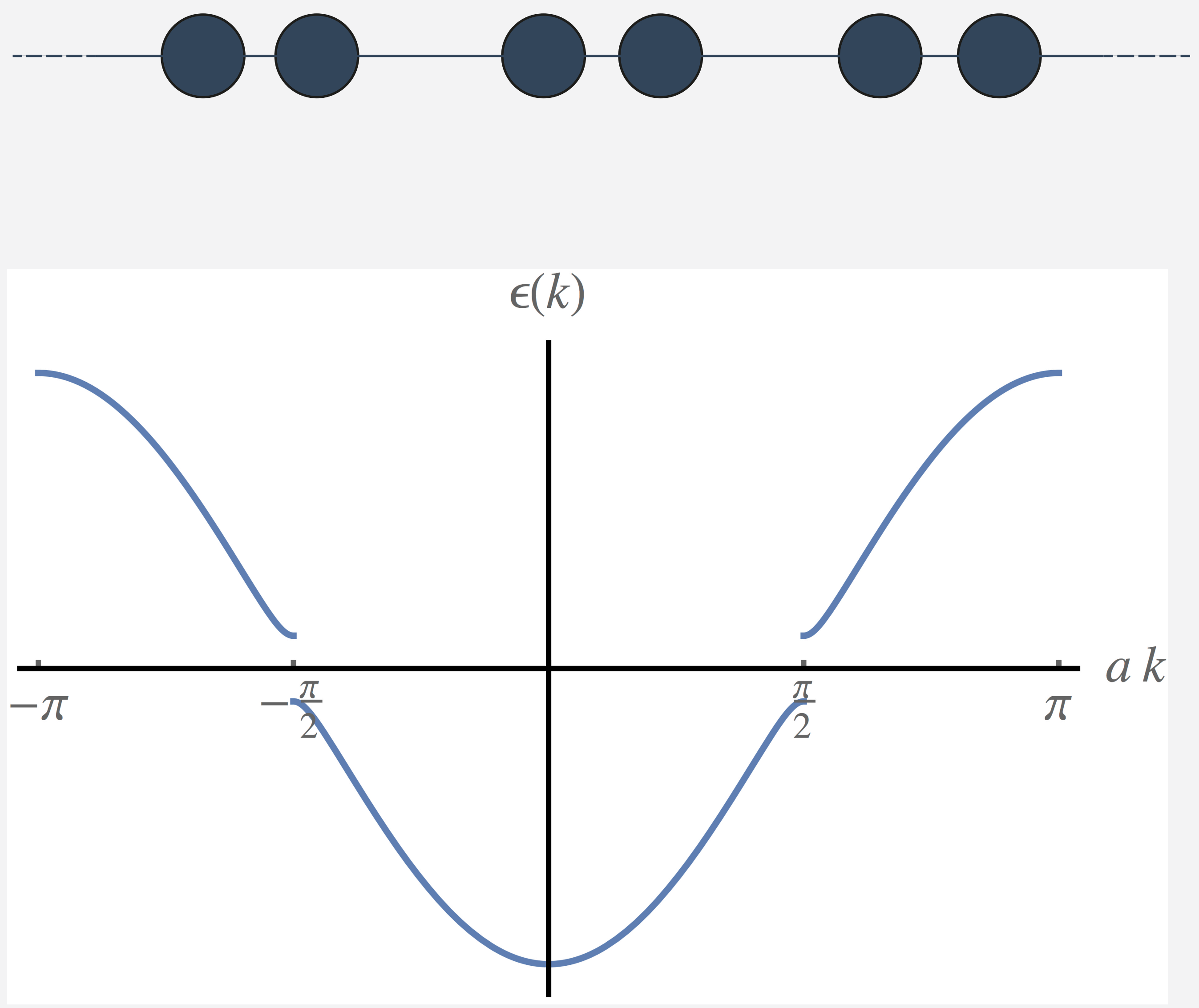

distorted 1D lattice

- **solving the Schrödinger equation for a periodic potential in one dimension results in energetically more stable solution for bond length alternation**
- **energy gained by opening a band gap and thus lowering the filled energy levels is larger than the energy lost by the dimerization of carbon atoms**

Degenerate Ground States In Poly(acetylene)

- poly(acetylene) is the only π-conjugated polymer with two equivalent resonance structures

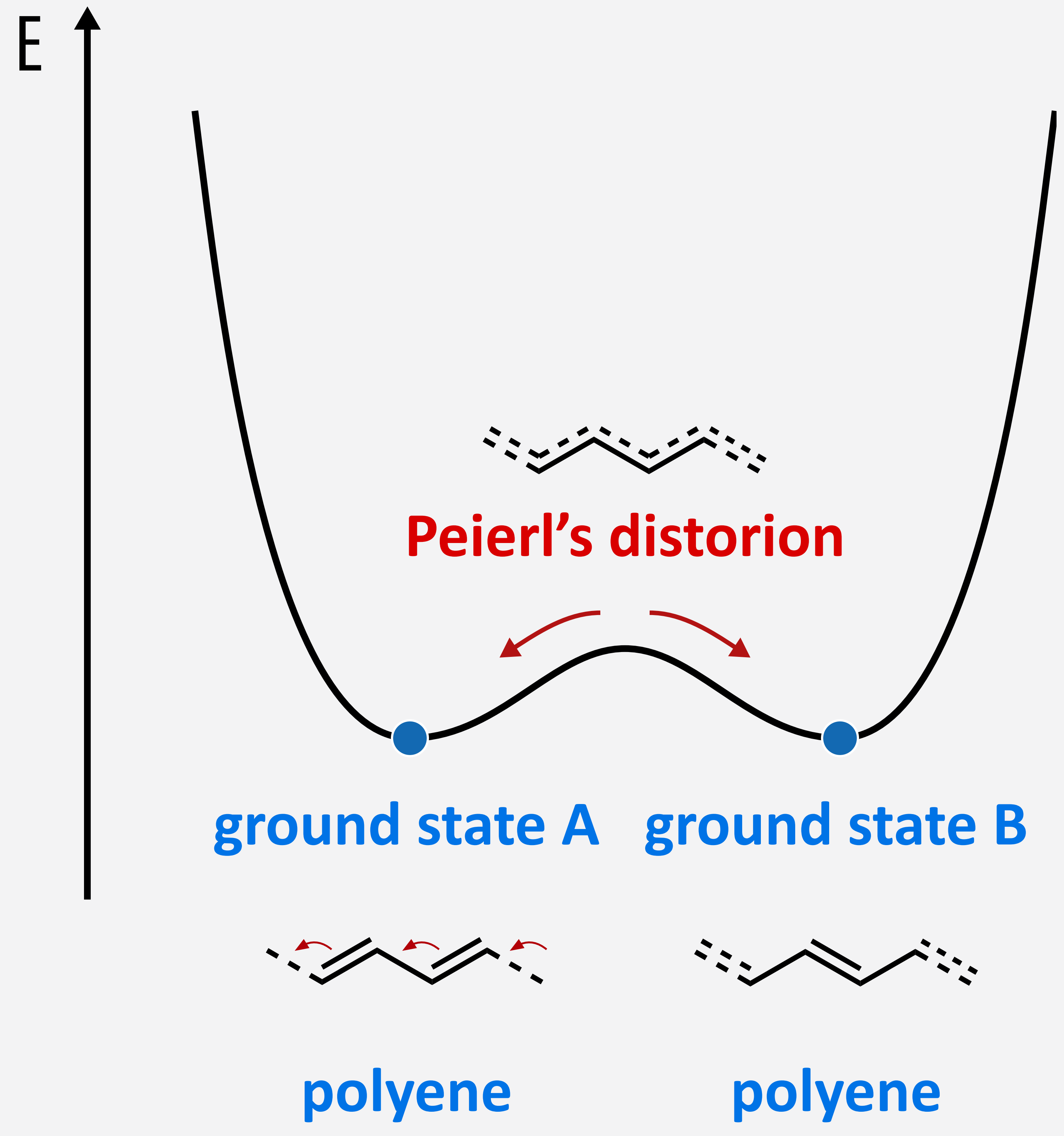

- **poly(acetylene) has two energetically & geometrically equivalent, *degenerate* ground states**
- **poly(acetylene) is unique in the sense that it has solitons as charge carriers**

“Spontaneous” Formation of Neutral Solitons in Poly(acetylene)

- at finite temperature, “lattice defects” at domain boundaries result in neutral solitons

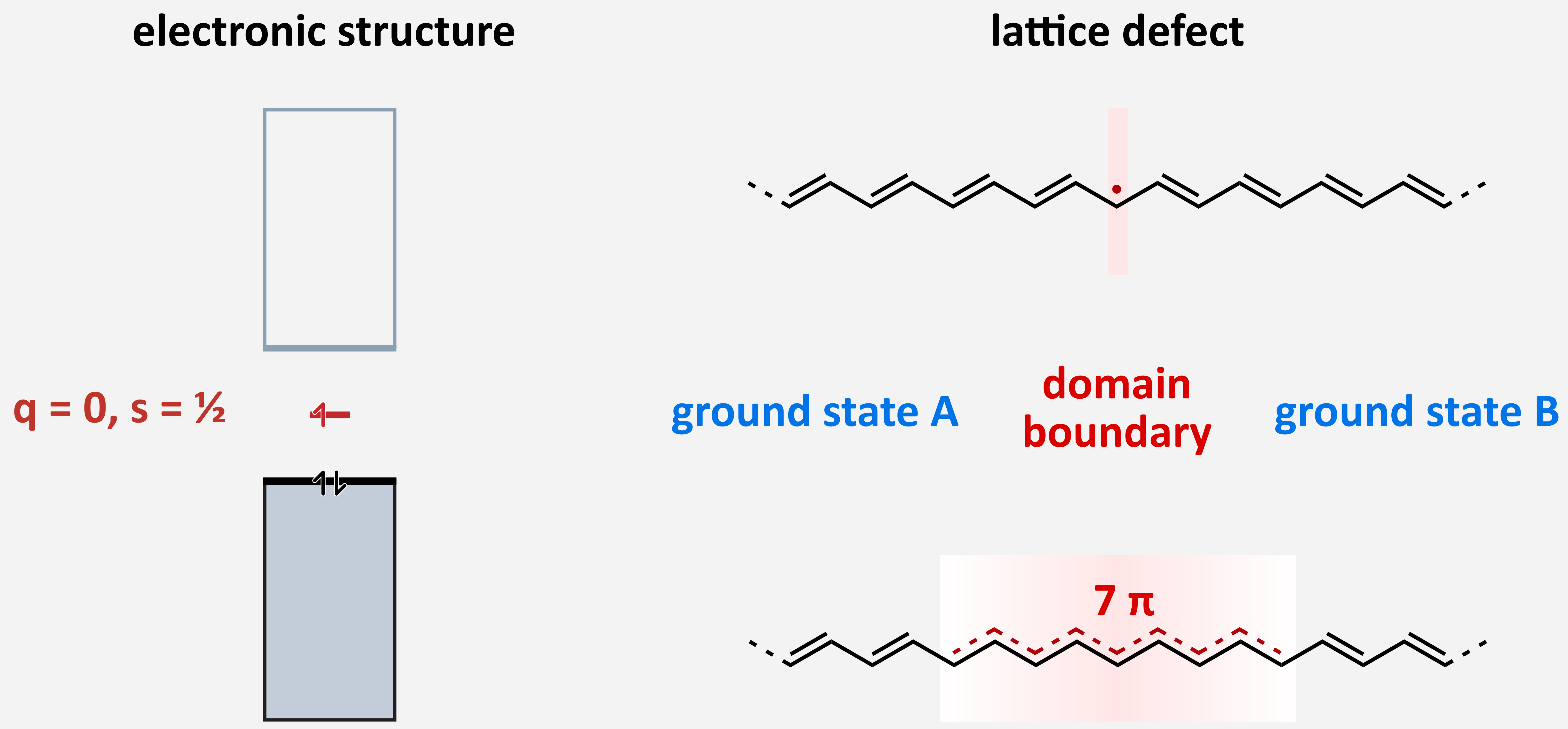

- **lattice distortion results in defect energy level in band gap with limited delocalization**
- **neutral solitons are particles with spin *s* = ½ and charge *q* = 0 plus lattice distortion**
- **organic chemistry view: neutral solitons are radicals**
- **neutral solitons cannot contribute to conduction, but are easily oxidized/reduced**

SSH Model of the Soliton

- Electron Spin Resonance (ESR) spectroscopy (based on Zeeman splitting $\Delta E = m_s g_e \mu_B B_0$)
  - g factor of g_e = 2.0026, similar to a free electron (2.0023)
  - spin density of $1.23 \cdot 10^{19}$ cm^{-3} or 1 soliton per 3200 carbon atoms (vs $MnSO_4 \cdot H_2O$)
  - spin density insensitive to NH_3 vapor (used to quench inadvertent charge carriers)
  - Lorentzian peak shape, no hyperfine structure, line narrowing at higher temperatures imply delocalization and thermally activated mobility of the soliton defect

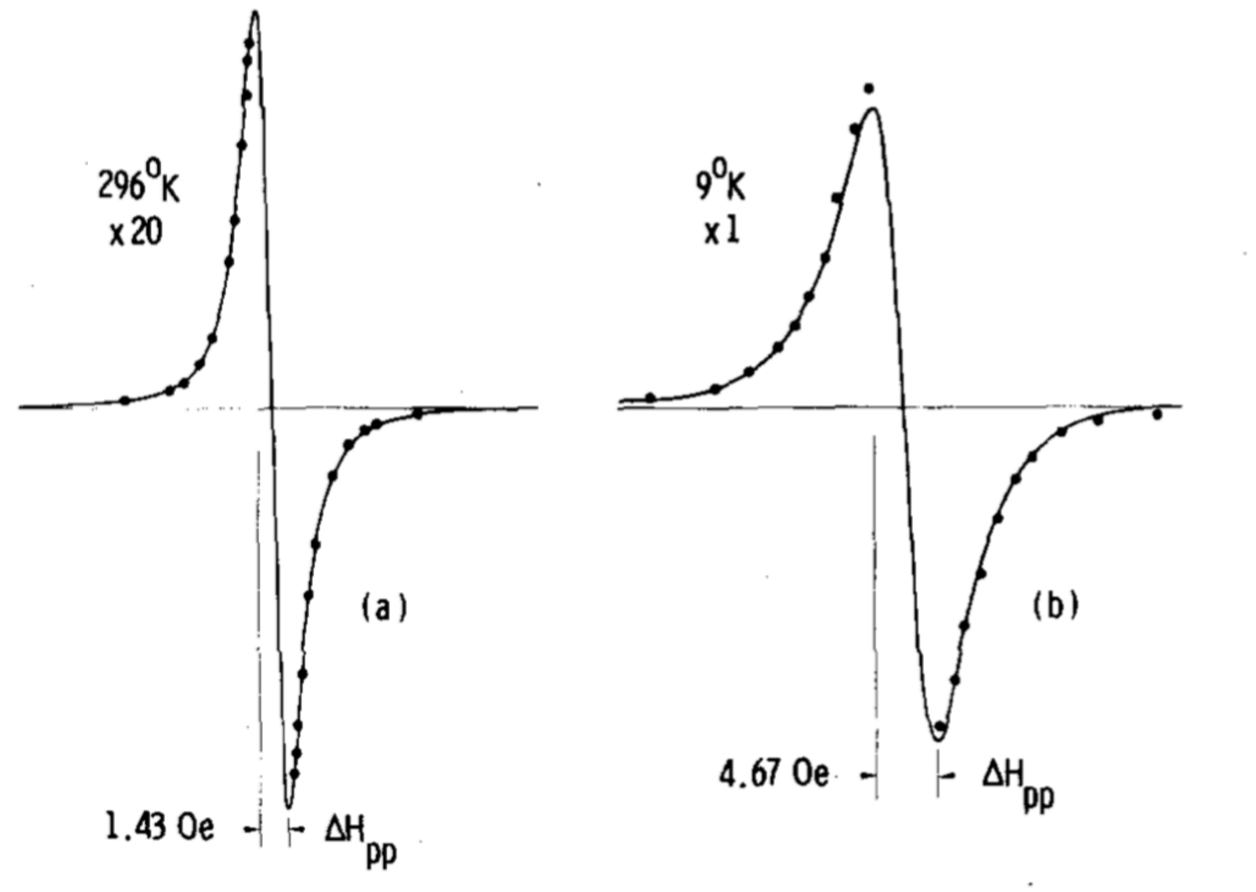

FIG. 1. ESR spectra (first derivative) of films of *trans*-$(CH)_x$ at 296 °K (a) and 9 °K (b). The circles show the theoretical lineshape based upon the peak-to-peak linewidth of the ESR spectra. (Magnetic field scales are not identical.)

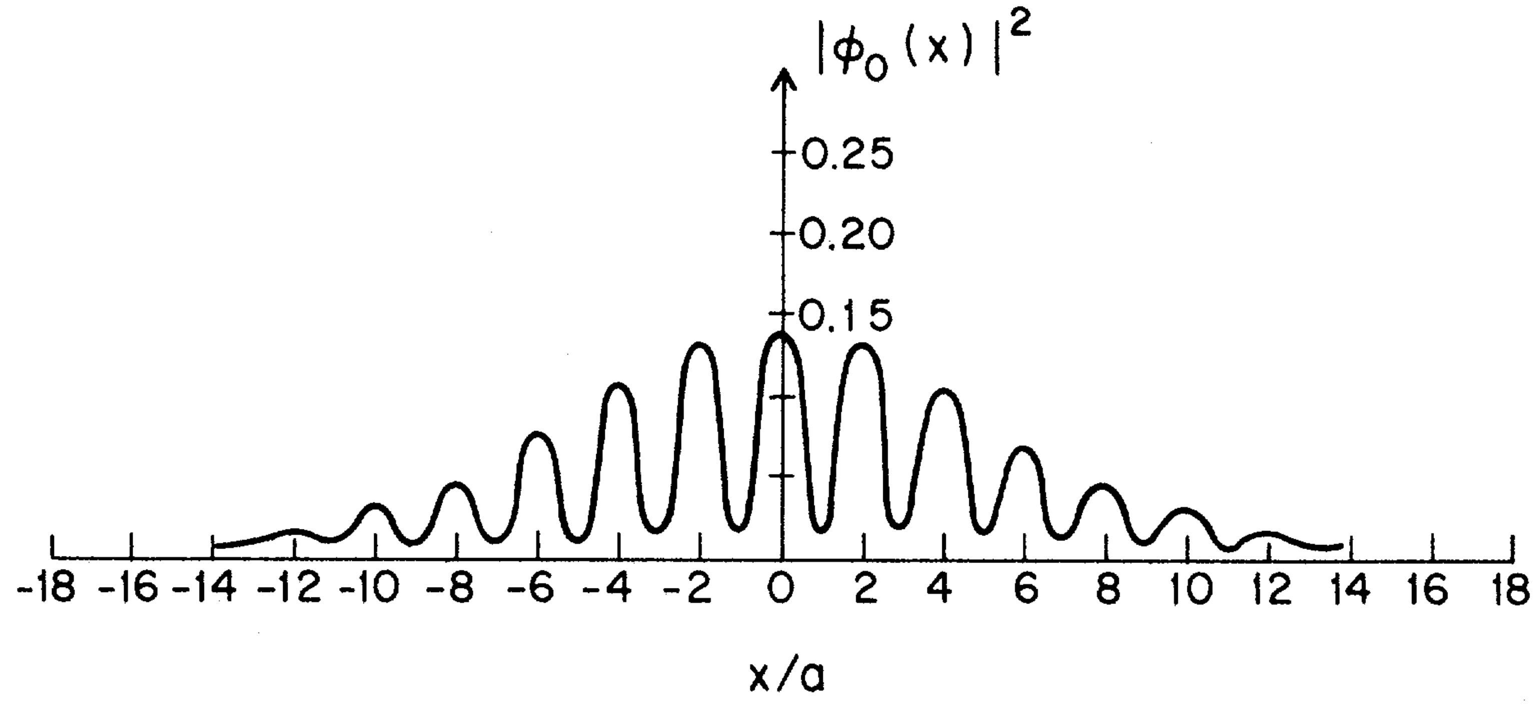

FIG. 3. Probability distribution of the localized electronic state at the center of the gap.

- **Electron-Nuclear Double Resonance (ENDOR): soliton delocalized over 7–9 carbon atoms**
- **Su-Schrieffer-Heeger (SSH) model: solitons are neutral defects with spin s = ½, charge q = 0**

Chemical Doping

- doping of poly(acetylene) with halogens or alkali metals

$$\text{polyacetylene} + \frac{3}{2}y\ \text{I}_2 \longrightarrow \text{polyacetylene}^{y+}\ (\text{I}_3^-)_y$$

$$\text{polyacetylene} + y\ \text{Na}^+\text{Naph}^{-\bullet} \longrightarrow \text{polyacetylene}^{y-}\ (\text{Na}^+)_y$$

Table I. Conductivity of Polycrystalline Polyacetylene and Derivatives (As-Grown Films)

Material	Conductivity, σ (Ω^{-1} cm^{-1}) (25 °C)
cis-$(CH)_x$[a,b]	1.7×10^{-9}
trans-$(CH)_x$[a,b]	4.4×10^{-5}
trans-$[(CH)(HBr)_{0.04}]_x$	7×10^{-4}
trans-$(CHCl_{0.02})_x$	1×10^{-4}
trans-$(CHBr_{0.05})_x$[c]	5×10^{-1}
trans-$(CHBr_{0.23})_x$[b,c]	4×10^{-1}
cis-$[CH(ICl)_{0.14}]_x$	5.0×10^{1}
cis-$(CHI_{0.25})_x$	3.6×10^{2}
trans-$(CHI_{0.22})_x$[b,c]	3.0×10^{1}
trans-$(CHI_{0.20})_x$[b]	1.6×10^{2}
cis-$[CH(IBr)_{0.15}]_x$	4.0×10^{2}
trans-$[CH(IBr)_{0.12}]_x$	1.2×10^{2}
trans-$[CH(AsF_5)_{0.03}]_x$	7×10^{1}
trans-$[CH(AsF_5)_{0.10}]_x$[b]	4.0×10^{2}
cis-$[CH(AsF_5)_{0.14}]_x$	5.6×10^{2}
trans-$[Na_{0.28}(CH)]_x$	8×10^{1}

[a] H. Shirakawa, T. Ito, and S. Ikeda, unpublished results; see ref 1–3. [b] Composition obtained by chemical analysis from Galbraith Laboratories, Inc. (sum of all elements is ~99.8–100.1%). [c] See ref 1–3.

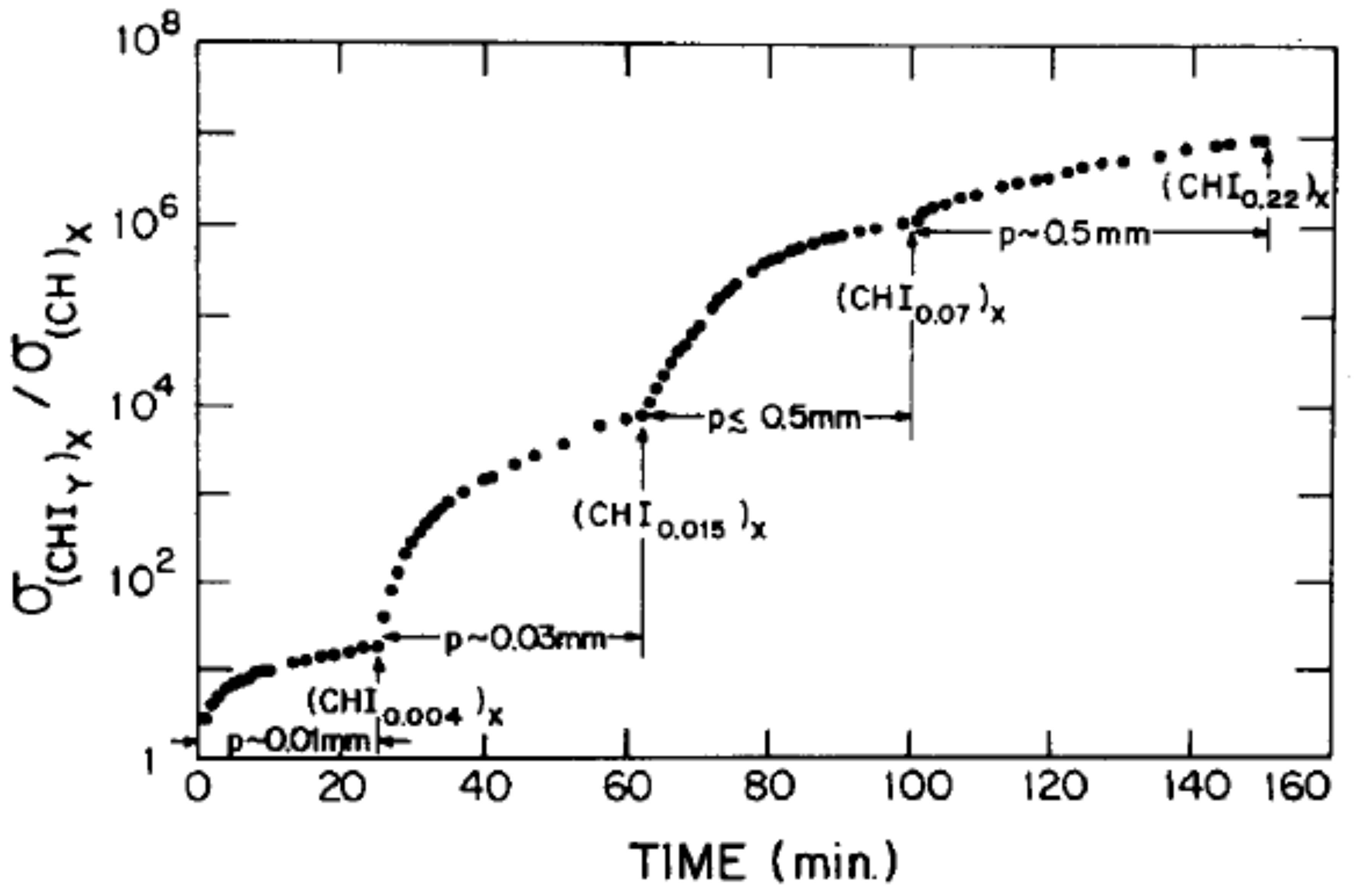

FIG. 3. Electrical conductivity (4-probe) of *trans*-$(CH)_x$ during doping reaction with iodine. The conductivity is normalized to that of the undoped sample.

- **chemical doping of poly(acetylene) results in up to 10^8-fold increase conductivity**

- chemically doped poly(acetylene) in the solid state becomes semiconducting or metallic

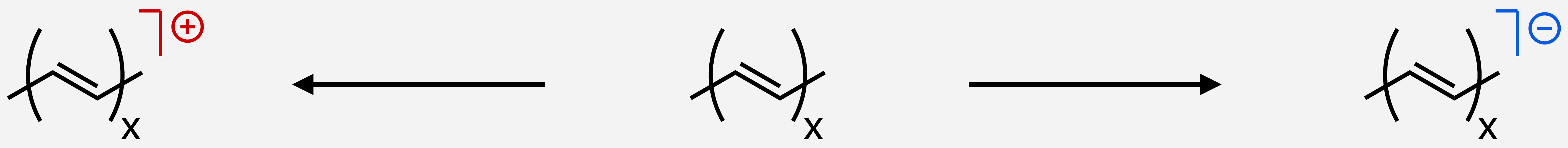

p-type doping	poly(acetylene)	n-type doping
good semiconductor	poor semiconductor	good semiconductor
I_2, AsF_5, SbF_5		**Na, K, Li**
oxidant		reductant
single electron acceptor		single electron donor

- **different from inorganic semiconductor "impurity doping" (at ppm concentrations)**
- **"single electron transfer" oxidant/reductant, but must not induce follow-up reactions**
- **dopant applied at high concentrations (0.1–10 mol%), strongly disturbs structure/geometry**
- **conductivity & mobility increased by several orders of magnitude by chemical doping**

Formation of Positive or Negative Soliton Charge Carriers

- chemical doping converts neutral solitons into positive or negative soliton charge carriers

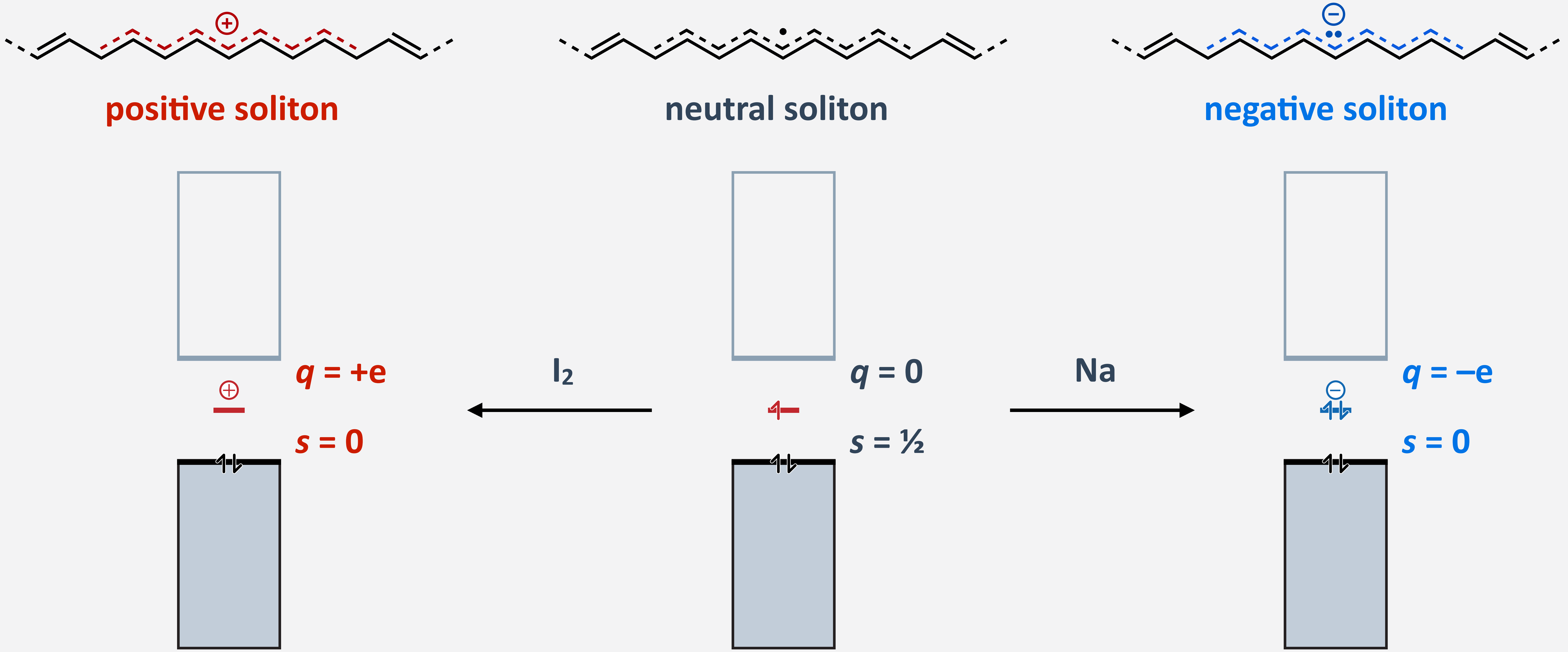

- **positive/negative solitons have no spin (s = 0) but carry a charge (q = ±e)**
- **organic chemistry view: carbocations or carbanions (delocalized over 7–23 carbon atoms)**
- **weakly doped poly(acetylene) is a semiconductor (isolated charges, limited delocalization)**
- **insulator-metal transition in strongly doped poly(acetylene) at about 10^{21} charges/cm^{-1}**

Doping-Induced Phase Transition

- sub-stoichiometric amounts of dopant, unlike impurity doping in inorganic semiconductors

undoped polyacetylene

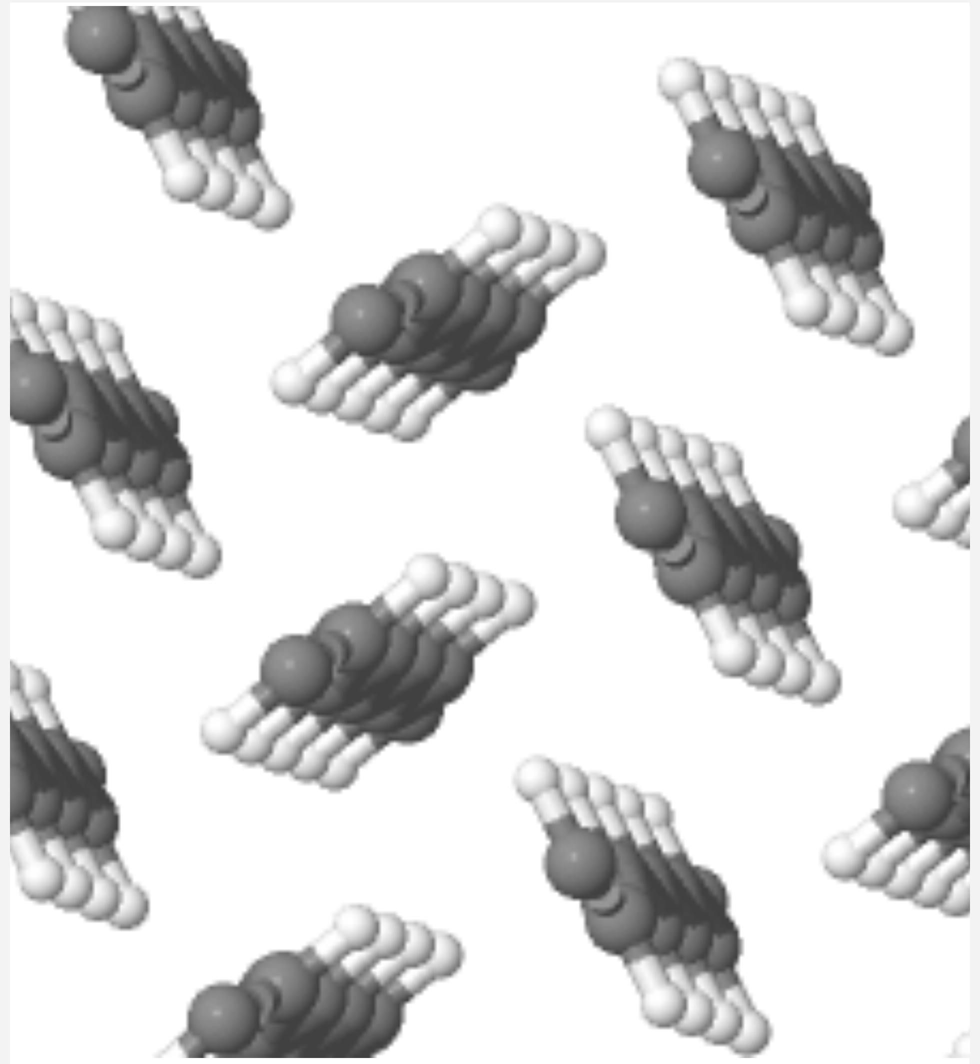

doping transition

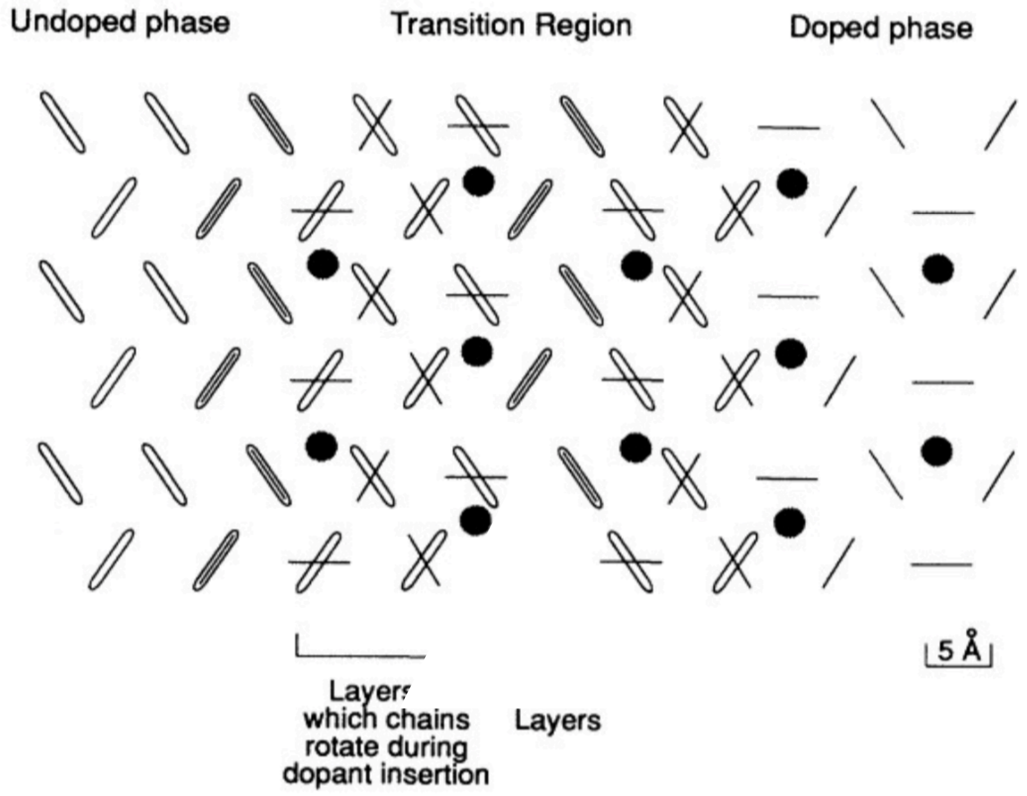

FIG. 4. Superposition of the lattices of undoped and lithium-doped polyacetylene in chain-axis projection. The open cigar-shaped boxes represent polyacetylene in the undoped phase. The lines represent the polyacetylene chains in the doped trigonal phase. The shaded circles are the Li^+ ions.

Na-doped polyacetylene

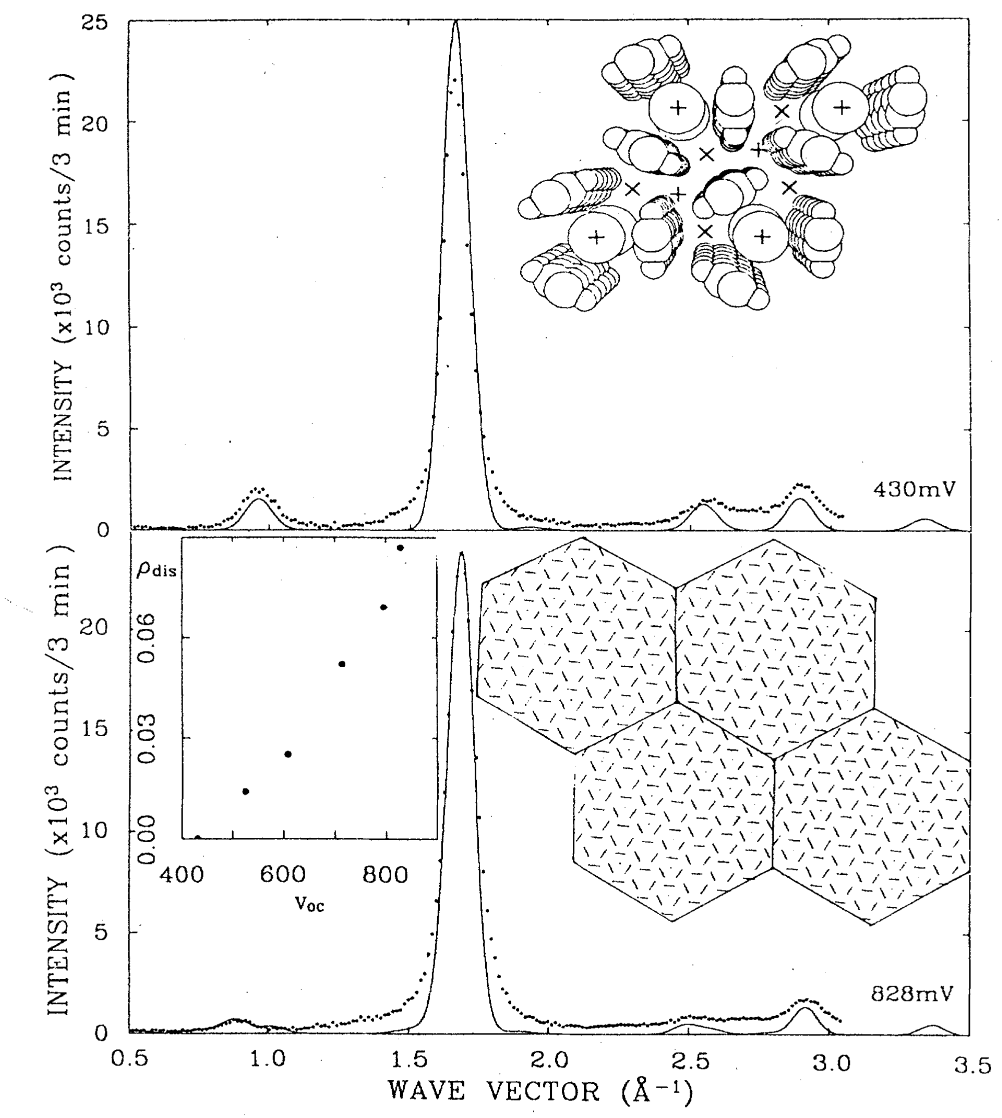

FIG. 7. Structure of Na-doped polyacetylene, $[(Na^+)_y(CH)^{+y}]_x$ (from Winokur *et al.*, 1987): (a) comparison between data (dots) and calculated diffraction profile (solid curve) for the commensurate $\sqrt{3}\times\sqrt{3}$ superlattice channel structure, $y\approx0.11$; (b) comparison between data (dots) and calculated diffraction profile (solid curve) for discommensurate-domain structure shown in the inset, $0.06<y<0.10$.

- **doping of polyacetylene results in phase transition to new materials with ion channels**

Charged Solitons

- charged solitons are supported by both theoretical models and experimental evidence

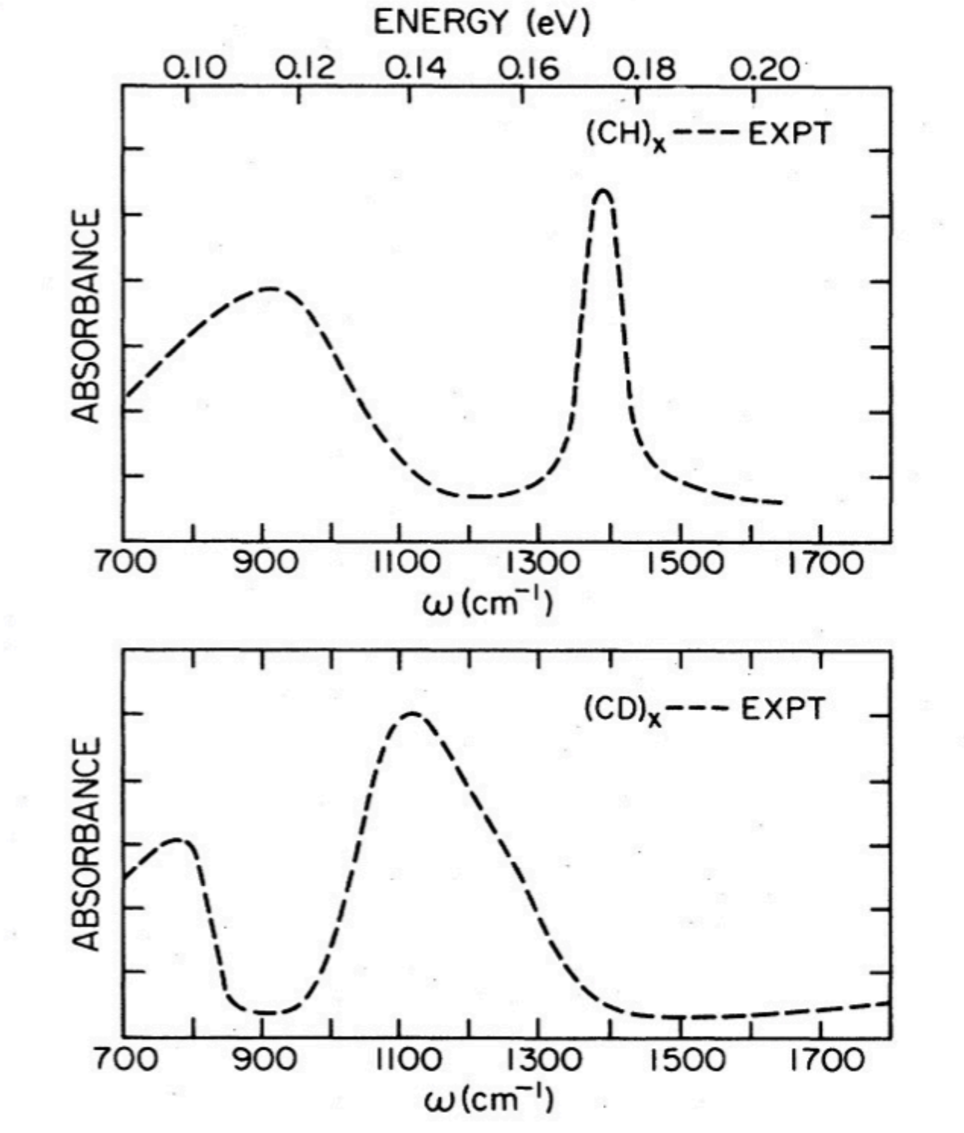

FIG. 32. Doping-induced infrared-active vibrational modes for *trans*-polyacetylene (from Etemad, Pron, *et al.*, 1981): (a) *trans*-$(CH)_x$; (b) *trans*-$(CD)_x$.

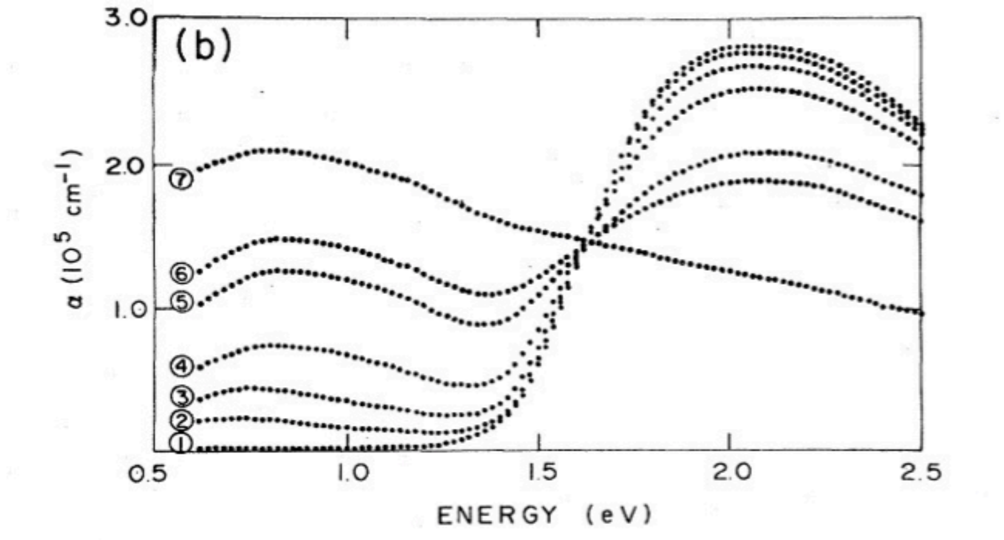

FIG. 34. Absorption spectra for neutral and doped *trans*-$(CH)_x$. (a) Absorption coefficient of *trans*-$(CH)_x$: ×, before doping; ●, after doping with a fraction of a percent by exposure to AsF_5 vapor (from Suzuki *et al.*, 1980). (b) *In situ* absorption curves for *trans*-$(CH)_x$ during electrochemical doping with $(ClO_4)^-$. The applied cell voltages (relative to Li) and corresponding concentrations are as follows: curve 1, 2.2 V ($y=0$); curve 2, 3.28 V ($y\sim0.003$); curve 3, 3.37 V ($y\sim0.0065$); curve 4, 3.46 V ($y\sim0.012$); curve 5, 3.57 V ($y\sim0.027$); curve 6, 3.64 V ($y\sim0.047$); curve 7, 3.73 V ($y\sim0.078$). From Feldblum *et al.*, 1982.

IR: additional vibrational modes upon doping

isotope-shift allows to link to modelling

UV-vis-NIR: appearance of absorptions within bandgap upon doping

broad features implies mid-bandgap band

- **charged soliton liquid undergoes first-order transition to a lattice of polaron-like defects**